

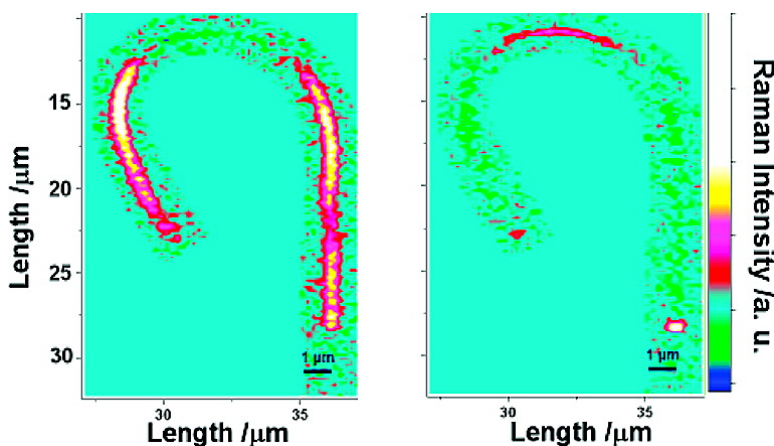
Communication

**Polarized Raman Confocal Microscopy of Single Gallium Nitride Nanowires**

Peter J. Pauzauskie, David Talaga, Kwanyong Seo, Peidong Yang, and Francois Lagugn-Labarthe

*J. Am. Chem. Soc.*, **2005**, 127 (49), 17146-17147 • DOI: 10.1021/ja056006b • Publication Date (Web): 17 November 2005

Downloaded from <http://pubs.acs.org> on March 25, 2009



**More About This Article**

Additional resources and features associated with this article are available within the HTML version:

- Supporting Information
- Links to the 9 articles that cite this article, as of the time of this article download
- Access to high resolution figures
- Links to articles and content related to this article
- Copyright permission to reproduce figures and/or text from this article

[View the Full Text HTML](#)

## Polarized Raman Confocal Microscopy of Single Gallium Nitride Nanowires

Peter J. Pauzauskie,<sup>†</sup> David Talaga,<sup>‡</sup> Kwanyong Seo,<sup>†,§</sup> Peidong Yang,<sup>\*,†</sup> and François Lagugné-Labarthe<sup>\*,‡</sup>

Department of Chemistry, University of California, Berkeley, and Materials Science Division, Lawrence Berkeley National Laboratory, Berkeley, California 94720, and Laboratoire de Physico-Chimie Moléculaire, UMR 5803 CNRS, Université Bordeaux I, 351 cours de la Libération, 33405 Talence Cedex, France

Received September 1, 2005; E-mail: p\_yang@berkeley.edu; f.lagugne@lpcm.u-bordeaux1.fr

One-dimensional semiconductor nanowires of the wide band gap semiconductor gallium nitride (GaN) are prime candidates for future nanoscale devices such as short wavelength optoelectronic devices, high-power/temperature electronics, or sensors for biological applications.<sup>1–3</sup> The electrical and optical properties of nanowires depend heavily on their crystalline structure and composition.<sup>1,4</sup> Subsequently, it is important to measure their homogeneity and composition at the level of single wires and to correlate these with the nanowire dimensions and optical properties.<sup>5</sup> In this context, optical microscopy and spectroscopy are able to provide information that goes far beyond visualizing the physical shape of materials. As demonstrated for the study of single carbon nanotubes,<sup>6,7</sup> Raman scattering is very helpful to probe the mechanical stress, thermal history, phonon confinement, and lattice dynamics, correlating optical spectra with the nanowire's crystallographic anisotropy and geometry. Raman confocal microscopy has a spatial resolution of roughly half the excitation wavelength, thus far limiting its use for the characterization of aggregated bundles of nanowires, and, as far as we know, far-field characterization of an individual nanowire together with polarization analyses has not yet been reported.<sup>8,9</sup>

In the present work, polarized Raman measurements were conducted locally with a confocal microscope (Horiba Jobin-Yvon Labram HR800) in conjunction with a high-resolution piezoelectric stage (PI) for accurate and reproducible positioning in order to characterize GaN nanowires that have their  $\bar{c}$  axis either along or perpendicular to their growth direction. Different sets of polarization input and output were used to assign unambiguously the phonon modes of the crystalline structures. Raman spectra under the polarization configurations  $Y(ZZ)\bar{Y}$ ,  $Y(XX)\bar{Y}$ , and  $Y(XZ)\bar{Y}$  are shown in Figure 1. The excitation wavelength was fixed at  $\lambda = 514.5$  nm, and the input/output polarizations were selected with a half-waveplate and a polarizer, respectively. The nanowire has a diameter of 170 nm and was aligned so that the Z polarization direction matches the growth direction (i.e., the  $\bar{c}$  axis for the  $\langle 001 \rangle$  orientation) of the nanowire.

As reported by various authors for thin films<sup>10,11</sup> and for collections of nanowires,<sup>8,12</sup> GaN that crystallizes in the hexagonal wurtzite-type structure belongs to the space group  $C_{6v}^4$  and has two formula units per primitive cell. According to the factor group analysis, the Raman active modes are  $1A_1 + 1E_1 + 2E_2$ , while  $2B_2$  modes are silent. Since the wurtzite structure is noncentrosymmetric, both  $A_1$  and  $E_1$  modes split into longitudinal optical (LO) and transverse optical (TO) components. For a single GaN nanowire, four main signals are observed in Figure 1 at 142, 530, 558, and 568  $\text{cm}^{-1}$ , and they can be assigned to  $E_2(\text{low})$ ,  $A_1(\text{TO})$ ,  $E_1(\text{TO})$ , and  $E_2(\text{high})$  symmetry type modes, respectively. In the  $Y(XZ)\bar{Y}$  configuration, only the  $E_1(\text{TO})$  mode is expected, and the

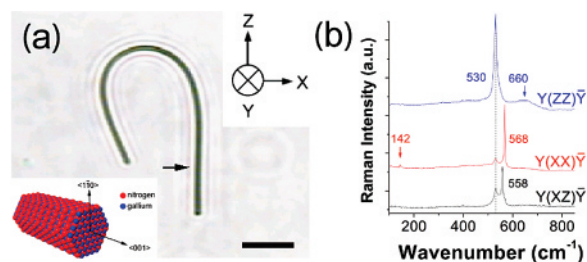


**Figure 1.** (a) Video image and polarization configuration of the Raman instrument. The  $Y$  direction is labeled for the incoming laser where  $Z$  and  $X$  define polarizations parallel and perpendicular to the wire growth direction, respectively. Scale bar =  $5 \mu\text{m}$ . Inset: Illustration of crystallographic directions in wurtzite GaN lattice. (b) Polarized Raman spectra of the GaN nanowire in the  $Y(ZZ)\bar{Y}$ ,  $Y(XX)\bar{Y}$ , and  $Y(XZ)\bar{Y}$  polarization configurations. The term  $Y(XZ)\bar{Y}$  indicates the incoming laser approaches from the  $Y$  direction and is polarized in  $X$ , while signal is collected with  $Z$  polarization in the opposite  $Y$  direction. The arrow in (a) indicates the area where the spectra shown in (b) have been recorded.

peak at  $530 \text{ cm}^{-1}$  ( $A_1(\text{TO})$ ) denotes a polarization leak. The broad peak mode at  $660 \text{ cm}^{-1}$  is assigned to a defect state with an energy close to the  $A_1(\text{LO})$  or to the first overtone of a  $B_1$  silent mode. This demonstrates that confocal techniques may be used as an easy, inexpensive, and rapid way to characterize the phase and growth direction of single nanowires.

Mapping of the nanowire was performed by recording step-spectra every 200 nm with an integration time of 1 s. A 100X NA = 0.9 microscope objective was used. Furthermore, no spectral shifts were observed with longer collection times, suggesting that possible laser heating is not affecting the crystal lattice. By intensity integration of the  $[509–552 \text{ cm}^{-1}]$  spectral domain around the  $A_1(\text{TO})$  mode ( $530 \text{ cm}^{-1}$ ), the variations of the Raman signal over the full nanowire are investigated (Figure 2). The images show details with lateral resolution better than 200 nm and with a reasonable acquisition time of about 1 h for a complete polarized image. For the  $Y(ZZ)\bar{Y}$  polarization configuration, Figure 2a shows that the signal is maximum on the straight portions of the nanowire, while it disappears on the bent portion of the nanowire. The complementary image (Figure 2b) is obtained by integration of the  $E_2(\text{high})$  mode at  $568 \text{ cm}^{-1}$ . In the  $Y(XX)\bar{Y}$  polarization configuration, the opposite spectroscopic contrast is observed with a maximum signal of the  $568 \text{ cm}^{-1}$  mode in the straight portions of the wire as observed in Figure 2c and a maximum signal for the  $A_1$  mode in the horizontal part of the nanowire. Under these scattering configurations, the optical longitudinal phonon modes were not observed.

To complement these polarized spectra, we have also measured nonpolarized spectra of an isolated, horizontal GaN nanowire grown in the  $[1\bar{1}0]$  direction with its  $\bar{c}$  axis oriented perpendicular to that of growth. Due to cylindrical geometry of this nanowire, the angular position of  $\bar{c}$  relative to the substrate plane is not known (Figure

<sup>†</sup> University of California, Berkeley.

<sup>‡</sup> University of Bordeaux.

<sup>§</sup> Current address: Department of Chemistry, KAIST, Daejeon 305-701, Republic of Korea.

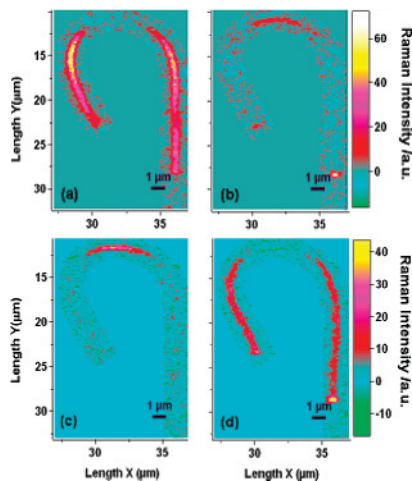


**Figure 2.** Polarized Raman images generated by integration of the [509–552  $\text{cm}^{-1}$ ] (a) and [558–575  $\text{cm}^{-1}$ ] (b) spectral ranges for  $Y(ZZ)\bar{Y}$  polarization configuration. Polarized Raman images generated by integration [509–552  $\text{cm}^{-1}$ ] (c) and [558–575  $\text{cm}^{-1}$ ] (d) spectral ranges for  $Y(XX)\bar{Y}$  polarization configuration.

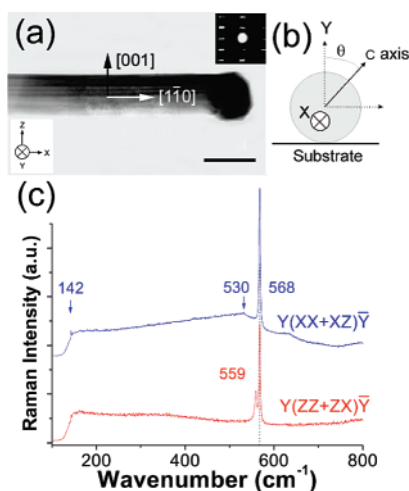


**Figure 3.** (a) GaN nanowire grown by chemical vapor transport with a cylindrical cross section in the  $[1\bar{1}0]$  direction. Scale bar = 100 nm. Inset is an electron diffraction pattern from the nanowire taken with a large diffraction aperture, illustrating growth direction. (b) Schematic showing possible orientations of transverse  $c$ -axis. (c) Raman polarized spectra with input polarization parallel ( $XX + XZ$ ) or orthogonal ( $ZZ + ZX$ ) to the growing direction.

3b). For  $Y(XX + XZ)\bar{Y}$  spectra (Figure 3c), the input polarization is along the growth direction, and no analyzer was used. Only the two  $E_2$  modes (low and high) can be observed at 143 and 568  $\text{cm}^{-1}$ , respectively. With an orthogonal polarization input relative to the growth direction,  $Y(ZZ + ZX)\bar{Y}$ , only  $E_1$  and  $E_2(\text{high})$  at 559 and 568  $\text{cm}^{-1}$ , respectively, can be observed. It is noteworthy that the  $A_1(\text{TO})$  mode is not clearly defined, and only a broad background can be observed in Figure 3c.

These observations exclude an orientation of the  $\bar{c}$  axis in the perpendicular direction relative to the substrate plane (i.e., along the propagation direction of the probe beam) where  $A_1$  mode should be observed along with  $E_2$ . Also, the  $\bar{c}$  axis cannot be oriented along

the substrate plane where the  $A_1$  mode should also be observed together with the  $E_1$ . This is certainly due to a peculiar orientation of the  $\bar{c}$  axis which is tilted with respect to the substrate plane, possibly by as much as  $45^\circ$ . In addition, for the  $[001]$  nanowire, the  $A_1$  mode clearly is very weak compared to the intensity of the  $E_2(\text{high})$  mode. This is an additional way to account for the absent  $A_1$  mode since only the  $E_2$  modes are expected to be dominant for such a configuration. This emphasizes the tremendous advantage of polarized Raman spectroscopy enabling the rapid assignment of the crystalline phase, growth direction, and also the probable orientation of its radial crystallographic axes as it rests horizontal on a surface. This information is critical for future photonics integration.<sup>13</sup>

In summary, we have performed a complete polarized Raman study of single GaN nanowires using a confocal microscope together with a high-resolution stage. The Raman assignments compare well to those from thin films, and studies on epitaxially grown nanowires show mainly first-order Raman effects. The high spatial resolution of the Raman confocal instrument together with a piezoelectric stage demonstrates unambiguously the possibility to image the Raman signal of nanomaterials with spectral-map features smaller than 200 nm. Furthermore, polarization measurements demonstrate the ability to gain information on the nanowire's phase, growth direction, and radial crystallographic orientation. In the future, the use of a high-resolution spectrometer should enable observation of stress-induced shifts and crystallinity modifications at various growing temperatures for individual nanostructures.

**Acknowledgment.** The authors thank the France–Berkeley Fund for the support of this work. F.L.L. and D.T. are indebted to the CNRS and to the Région Aquitaine for financial support. P.J.P. thanks the NSF for a graduate research fellowship. Work at the Lawrence Berkeley National Laboratory was supported by the Office of Science, Basic Energy Sciences, Division of Materials Science of the U.S. Department of Energy.

**Supporting Information Available:** Experimental details. This material is available free of charge via the Internet at <http://pubs.acs.org>.

## References

- (1) Pauzauskie, P.; Kuykendall, T.; Zhang, Y.; Goldberger, J.; Sirbully, D.; Denlinger, J.; Yang, P. *Nat. Mater.* **2004**, *3*, 524.
- (2) Choi, H.; Johnson, J.; He, R.; Lee, S.-K.; Kim, F.; Pauzauskie, P.; Goldberger, J.; Saykally, R.; Yang, P. *J. Phys. Chem. B* **2003**, *107*, 8721.
- (3) Huan, Y.; Duan, X.; Cui, Y.; Lieber, C. *Nano Lett.* **2002**, *2*, 101.
- (4) Bae, S. Y.; Seo, H. W.; Park, J.; Yang, H.; Kim, H.; Kim, S. *Appl. Phys. Lett.* **2003**, *82*, 4564.
- (5) Wang, J.; Gudiksen, M. S.; Duan, X.; Cui, Y.; Lieber, C. M. *Science* **2001**, *293*, 1455.
- (6) Dresselhaus, M. S.; Dresselhaus, G.; Jorio, A.; Souza Filho, A. G.; Pimenta, M. A.; Saito, R. *Acc. Chem. Res.* **2002**, *35*, 1070.
- (7) Hartschuh, A.; Sanchez, E.; Xie, X. S.; Novotny, L. *Phys. Rev. Lett.* **2003**, *90*, 95503.
- (8) Liu, H.-L.; Chen, C.-C.; Chia, C.-T.; Yeh, C.-C.; Chen, C.-H.; Yu, M.-Y.; Keller, S.; DenBaars, S. P. *Chem. Phys. Lett.* **2001**, *345*, 245.
- (9) Liu, J.; Meng, X.-M.; Jiang, Y.; Lee, C.-S.; Bello, I.; Lee, S.-T. *Appl. Phys. Lett.* **2003**, *83*, 4241.
- (10) Harima, H. *J. Phys.: Condens. Matter* **2002**, *14*, R967.
- (11) Azuhata, T.; Sota, T.; Suzuki, K.; Nakamura, S. *J. Phys.: Condens. Matter* **1995**, *7*, L129.
- (12) Zhang, J.; Zhang, L.; Jiang, F.; Yang, Y.; Li, J. *J. Phys. Chem. B* **2005**, *109*, 151.
- (13) Sirbully, D. J.; Law, M.; Pauzauskie, P.; Yan, H. Q.; Maslov, A. V.; Knutsen, K.; Ning, C. Z.; Saykally, R. J.; Yang, P. D. *Proc. Natl. Acad. Sci. U.S.A.* **2005**, *102*, 7800.

JA056006B